Journal of Environmental and Development Studies - JEDS
Journal homepage: https://talenta.usu.ac.id/jeds

Performance Analysis of an Air-Based PV/T System in a Greenhouse Based on Indoor and Outdoor Test Chamber Temperature Comparison

Fiky Setiawan*[1], Ayu Zahra Chandrasari[1], & Tinton Dwi Atmaja[2], & Ahmad Rajani[2]

[1]*Department of Mechanical Engineering, Faculty of Engineering, Universitas Widyatama, Bandung 40125, Indonesia*

[2]*Research Center for Energy Conversion and Conservation, National Research and Innovation Agency (BRIN), Banten 15314, Indonesia*

*Corresponding Author: setiawan.7698@widyatama.ac.id

ARTICLE INFO

Article history:
Received 08 July 2026
Revised 30 July 2026
Accepted 01 August 2026
Available online 01 September 2026

E-ISSN: 2745-4592

How to cite:
Putra S. J., Chandrasari A. Z., Rajani A. Experimental Study on the Effect of Zigzag Configuration of Paraffin Wax-Filled Aluminum Containers on the Thermal Performance of a Photovoltaic Thermal System. Journal of Environmental and Development Studies 2026. 7(2):019-029

http://doi.org/10.32734/jeds.v7i2.26298

ABSTRACT

This study analyzes the thermal behavior of an air-based photovoltaic thermal (PV/T) system integrated with a greenhouse under tropical outdoor conditions in Bandung, Indonesia. The integration extracts excess heat from photovoltaic panels, which typically degrades electrical performance and utilizes it to modify the agricultural microclimate. The experimental setup comprised a PV/T air collector, inlet fans, a connecting outlet duct, type-K thermocouples, DHT sensors, a pyranometer, an anemometer, and a data logger. Measurements were processed at 10-minute intervals from 09:00 to 15:00 across three observation days. The analysis emphasized solar radiation, PV/T component temperatures, mass flow rate, useful heat extraction, system thermal efficiency, and the comparison between the internal greenhouse temperature (DHT5-DHT7) and the external outdoor temperature (DHT8). The empirical results demonstrated an average solar radiation ranging from 676.84 W/m² to 768.65 W/m² across the observation days. The average outlet-inlet air temperature difference ranged consistently from 5.81°C to 6.36°C. Using the measured outlet velocity and duct area, the calculated air mass flow rate was 0.0774 kg/s. Consequently, the system generated an average useful thermal output of 467.85 W and achieved an average thermal efficiency of 25.24%. This effective heat transfer resulted in the internal greenhouse temperature remaining significantly higher than the outdoor ambient temperature by an average margin of 4.05°C to 4.73°C. These findings conclusively indicate that the active PV/T hot air flow, combined with the greenhouse enclosure effect, substantially governed the thermal conditions inside the test chamber, providing a viable thermal management strategy.

Keywords: Air Collector, Greenhouse, Outdoor Temperature, Photovoltaic Thermal, Solar Radiation.

1. Introduction

The continuously increasing energy demand drives the development of renewable energy systems that can be utilized directly in the productive sector. Solar energy is one of the most relevant energy sources to be studied in Indonesia due to its relatively high availability throughout the year. In practice, photovoltaic panels not only generate electricity but also experience a temperature increase, as a portion of the received radiation is converted into heat. This temperature rise can decrease the electrical performance of the panels, thus requiring an approach capable of extracting heat from the panels and utilizing it as thermal energy (Fudholi et al., 2019).

Photovoltaic thermal (PV/T) systems were developed to combine the functions of a photovoltaic and a thermal collector into a single unit. In air-based PV/T systems, air as the working fluid is channeled through the collector duct so that heat from the panels and the absorber can be carried to the utilization space. This concept allows the panels to continue functioning as electricity generators, while the heat that was initially a thermal loss can be utilized as hot air for further applications (Fudholi et al., 2021).

The performance of air-based PV/T systems is determined not only by solar radiation but also by the inlet and outlet air temperatures, collector component temperatures, air flow velocity, and the air duct's capacity to transfer heat. Therefore, testing air-based PV/T systems requires simultaneous recording of radiation and temperature responses to determine whether the collector genuinely increases the outlet air temperature compared to the inlet (Dunne et al., 2023).

The integration of PV/T with a greenhouse is essential because the hot air from the collector actively modifies the microclimate conditions of the planting space. While existing literature has extensively explored PV/T-based greenhouse systems for general ventilation and heating applications (Gorjian et al., 2021; Jadallah et al., 2020), there remains a critical theoretical gap regarding the dynamic isolation of the system's thermal contribution under fluctuating tropical climates. Evaluating PV/T performance strictly through isolated collector efficiency fundamentally overlooks the thermal retention dynamics of the greenhouse envelope. Consequently, a direct indoor-outdoor temperature comparison is theoretically imperative. This specific comparative configuration isolates the thermal energy actively injected by the PV/T system from passive natural ambient heating, thereby defining its exact efficacy as a microclimate actuator.

Addressing this gap, the objective of this study is to comprehensively analyze the thermodynamic performance of an air-based PV/T system integrated with a greenhouse, utilizing three days of experimental data. This evaluation goes beyond descriptive temperature gradients by explicitly calculating the mass flow rate, useful heat transfer, and system thermal efficiency to establish its concrete engineering viability. The analysis systematically encompasses solar radiation intensity, the temperature response of the PV/T components, the outlet-inlet air temperature difference, and the dynamic indoor-outdoor greenhouse temperature comparison. To ensure measurement accuracy, the internal greenhouse temperature is calculated from the average of the DHT5, DHT6, and DHT7 sensors, while the DHT8 sensor records the external ambient temperature. By integrating these comprehensive thermal and thermodynamic parameters, this study aims to determine the actual capacity of the PV/T system to function as an active space heater and microclimate controller for agricultural applications (Al-Waeli et al., 2021; Zhou et al., 2025).

2. Method

2.1 Equipment Configuration and Airflow

The system used is an air-based PV/T with a forced-flow configuration. Ambient air enters the collector through an inlet fan on the front side of the PV/T, then passes through the duct space beneath the panels, absorbing heat from both the panels and the absorber. The air that has increased in temperature is channeled through an outlet duct to the greenhouse. On the greenhouse side, the air enters the test chamber and forms an internal circulation before the thermal condition of the space is read by the DHT5-DHT7 sensors. The outdoor reference temperature is recorded using the DHT8 sensor. The research flowchart is shown in Figure 1.

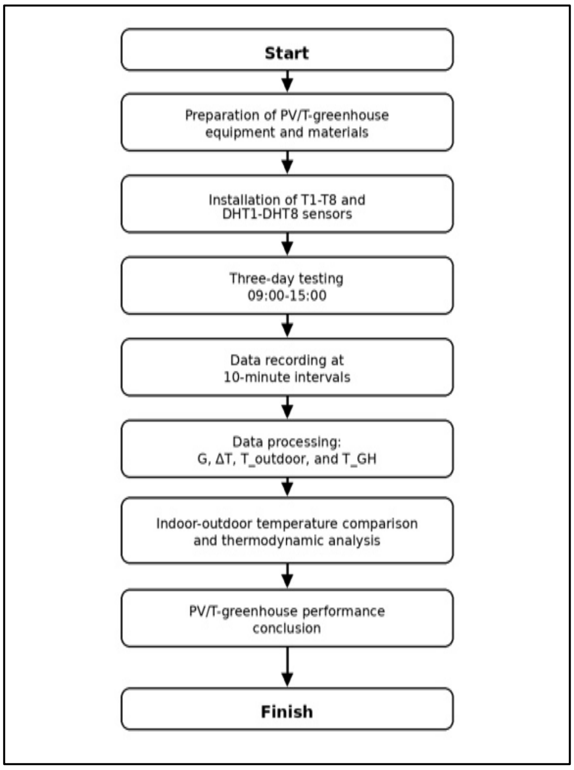

Figure 1. Flowchart of the PV/T-Greenhouse system research from preparation to conclusion.

A three-dimensional design model is used as a reference for the positions of the PV/T collector, air ducts, greenhouse, fans, and sensor points. The design illustrates the connection between the PV/T module, the outlet duct, and the greenhouse as the airflow receiving space. The design model is presented in Figure 2, while the actual equipment setup during testing is shown in Figure 3.

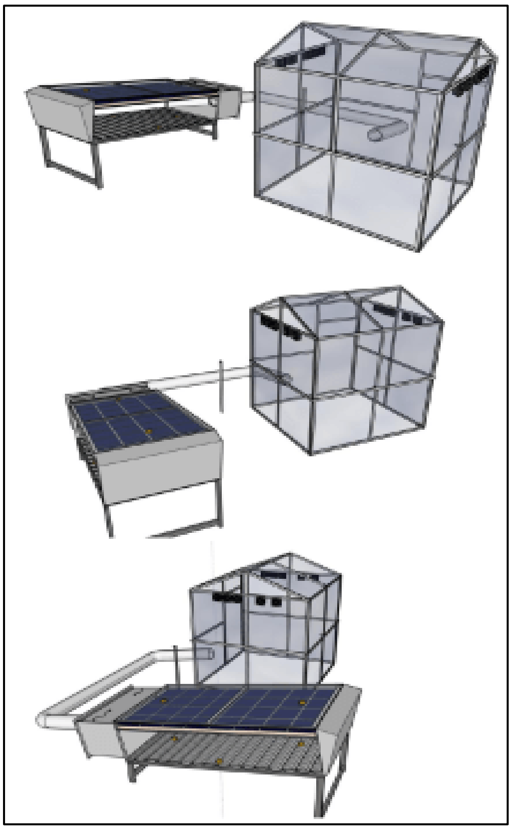

Figure 2. 3D design model of the PV/T-Greenhouse system and component positions.

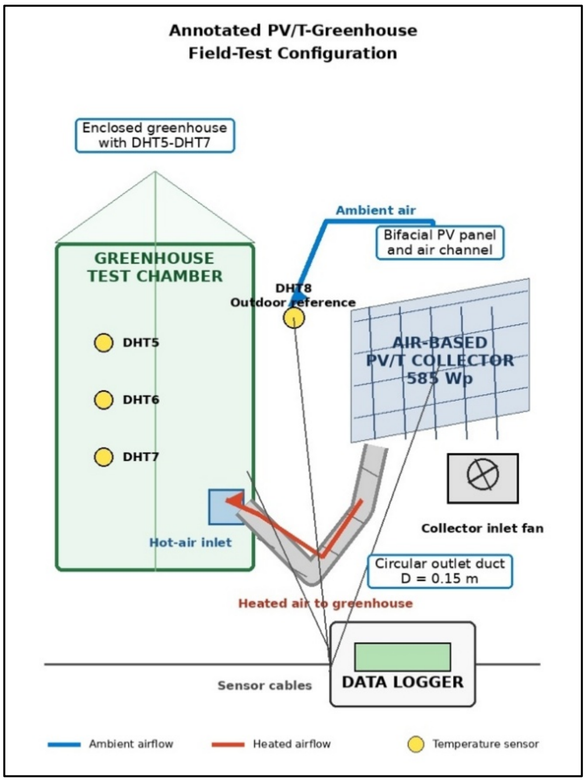

Figure 3. Annotated schematic of the PV/T-Greenhouse field-test configuration, including sensor positions and airflow direction.

2.2 Equipment, Materials, and Sensor Positions

The primary equipment consists of the PV/T panel, greenhouse, temperature sensors, solar radiation sensor, anemometer, fans, air ducts, and a data logger. Table 1 consolidates the specifications of the PV/T and greenhouse to provide a more concise overview of the equipment configuration.

Table 1. Specifications of the PV/T-Greenhouse research equipment and materials.

No.	Equipment/Material	Specification	Function
1	Air PV/T Panel	585 Wp PV/T, double-pass air collector; effective collector area 2.58 m²	Converts solar radiation and provides a heat transfer space for the air.
2	Greenhouse	Length 215 cm, width 196 cm, total height 238 cm, floor area ±4.21 m², volume ±9.3 m³	Test chamber and receiver of the hot airflow from the PV/T system.
3	PV/T Inlet Fan	Fan on the input side of the collector; measured outlet velocity is approximately 3.70 m/s	Pushes air through the PV/T collector.
4	Outlet Duct	Flexible circular duct from the PV/T outlet to the greenhouse; internal diameter 0.15 m; outlet area 0.01767 m²	Channels hot air from the collector to the greenhouse space.
5	Type-K Thermocouple	Points T1-T8	Measures the temperatures of the glass, bottom of the PV, and zinc absorber; PCM is not discussed in the main graphs.
6	DHT Sensor	Points DHT1-DHT8	Measures the inlet, outlet, indoor greenhouse, and outdoor greenhouse temperatures.
7	Radiation Sensor	Solar radiation reading range	Measures the solar radiation intensity received by the system.
8	Anemometer	Air/wind speed reading	Measures ambient wind speed and outlet air velocity.
9	Data Logger	Periodic data recording	Records sensor data during testing.

Table 2. Sensor positions and data processing parameters.

Sensor Group	Position	Processed Parameter
T1-T2	Glass/top surface of the collector	T_glass = average of T1 and T2
T3-T4	Bottom of the PV	T_PV_bottom = average of T3 and T4
T5-T6	PCM area/internal thermal space	Not displayed in the main graphs because the discussion is focused on the air-based PV/T system.
T7-T8	Zinc absorber	T_absorber = average of T7 and T8
DHT1-DHT2	Collector inlet air	T_in = average of DHT1 and DHT2
DHT3-DHT4	Collector outlet air	T_out = average of DHT3 and DHT4
DHT5-DHT7	Air inside the greenhouse	T_GH = average of DHT5, DHT6, and DHT7
DHT8	Environment outside the greenhouse	T_outdoor = DHT8

2.3 *Testing Procedure and Data Processing*

The testing was conducted over three days: Monday (08-06), Tuesday (09-06), and Wednesday (10-06). The processed data consists of minute-by-minute recordings with a 10-minute interval between 09:00 and 15:00. The recorded parameters include solar radiation, ambient wind speed, outlet air velocity, T1-T8 thermocouple temperatures, and DHT1-DHT8 temperatures. The data were then averaged and compared to determine the collector air temperature increase, the indoor-outdoor greenhouse temperature difference, and the temperature change trends relative to solar radiation.

2.4 Analytical Equations

The analytical equations used for data processing are presented in Table 3. Average sensor-temperature equations establish the spatial thermal mapping, while the thermodynamic equations calculate the mass flow rate, useful heat transfer, incident solar power, and thermal efficiency of the air-based PV/T system. The air properties were selected from standard heat-transfer and psychrometric data (Duffie et al., 2020; Geary, 2014). By incorporating the effective collector area, outlet cross-sectional dimensions, and measured outlet velocity, this mathematical approach quantifies the thermal energy conversion capability and the system's contribution to the greenhouse microclimate.

Table 3. Data processing equations and basic calculations for PV/T-Greenhouse.

No.	Parameter	Equation
1	Glass temperature	$T\_glass = (T1 + T2) / 2$
2	Bottom PV temperature	$T\_PV = (T3 + T4) / 2$
3	Absorber temperature	$T\_abs = (T7 + T8) / 2$
4	Inlet air temperature	$T\_in = (DHT1 + DHT2) / 2$
5	Outlet air temperature	$T\_out = (DHT3 + DHT4) / 2$
6	Indoor greenhouse temperature	$T\_GH = (DHT5 + DHT6 + DHT7) / 3$
7	Outdoor greenhouse temperature	$T\_outdoor = DHT8$
8	Collector air difference	$\Delta T\_air = T\_out - T\_in$
9	Air mass flow rate	$\dot{m} = \rho_a A_o V\_out$
10	Useful heat transfer	$Q_u = \dot{m} c_p (T\_out - T\_in)$
11	Incident solar power	$Q\_s = G A\_c$
12	Thermal efficiency	$\eta\_th = Q_u / (G A\_c) \times 100\%$

For the thermodynamic calculation, the air density was taken as 1.184 kg/m³ and the specific heat capacity of air as 1005 J/kg·K. The measured outlet air velocity was 3.70 m/s. Using the circular outlet duct internal diameter of 0.15 m, the outlet cross-sectional area was 0.01767 m². The effective PV/T collector area used in the incident solar energy calculation was 2.58 m². These parameters were applied to calculate the mass flow rate, useful heat transfer, and thermal efficiency.

3. Result

3.1 Solar Radiation Conditions During Testing

The changes in solar radiation intensity during the test are presented in Figure 4. The data are displayed at 10-minute intervals so that radiation fluctuations due to changing cloud conditions can be observed. The highest average radiation occurred on Monday at 768.65 W/m² with a maximum value of 1018 W/m². Tuesday had an average radiation of 710.22 W/m², while Wednesday had an average radiation of 676.84 W/m². The afternoon radiation decrease indicates that solar energy input to the PV/T system was unstable throughout the testing. This condition aligns with the characteristics of solar air collectors, which are highly influenced by changes in incoming radiation on air temperature rise and thermal efficiency (AL-Jaafari et al., 2025).

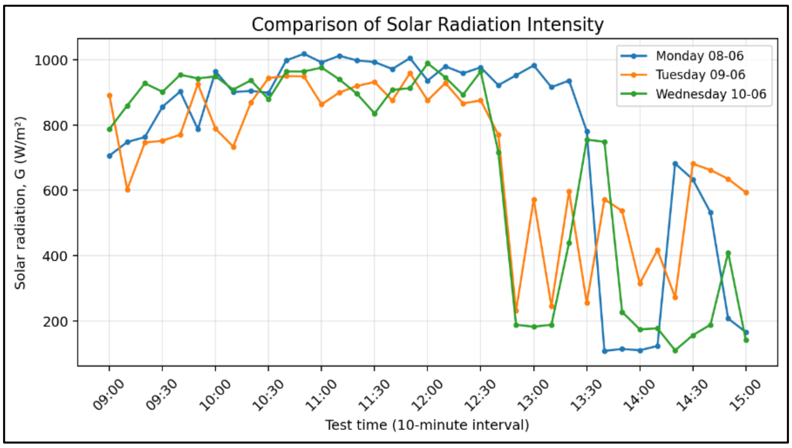

Figure 4. Comparison of minute-by-minute solar radiation intensity over the three days of testing.

3.2 Temperature Response of PV/T Components

Figure 5 presents the glass temperature, bottom PV temperature, and zinc absorber temperature to describe the air collector's thermal performance. Using Wednesday as an example, the bottom PV temperature was the highest because this part receives the direct heat effect of the panel. The absorber temperature remained below the bottom PV temperature but still increased as radiation increased. This indicates that the heat from the panel and the absorber acts as the source of air heating in the collector duct.

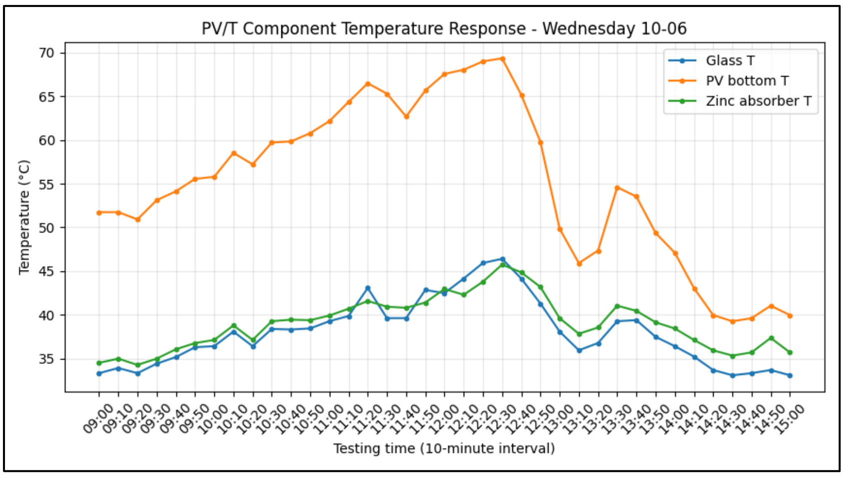

Figure 5. Temperature response of PV/T components on Wednesday 10-06.

3.3 PV/T Outlet-Inlet Air Temperature Difference

The air heating performance of the collector can be observed from the outlet-inlet air temperature difference. Figure 6 shows that air ΔT generally increased during periods of strong radiation and decreased when radiation weakened. The highest average air ΔT occurred on Monday at 6.36°C, while Tuesday and Wednesday produced 5.81°C and 5.87°C, respectively; the instantaneous maximum was 8.35°C on Wednesday. Using the measured outlet velocity of 3.70 m/s, an outlet area of 0.01767 m², and an air density of 1.184 kg/m³, the calculated mass flow rate was 0.0774 kg/s. With an air specific heat capacity of 1005 J/kg·K, the average useful heat transfer was 494.82 W on Monday, 452.03 W on Tuesday, and 456.70 W on Wednesday, giving an overall average of 467.85 W. Based on the effective collector area of 2.58 m², the corresponding average thermal efficiencies were 24.95%, 24.67%, and 26.15%, with an overall average of 25.24%. These results confirm that the forced airflow served as an active and continuous thermal energy source for modifying the greenhouse microclimate.

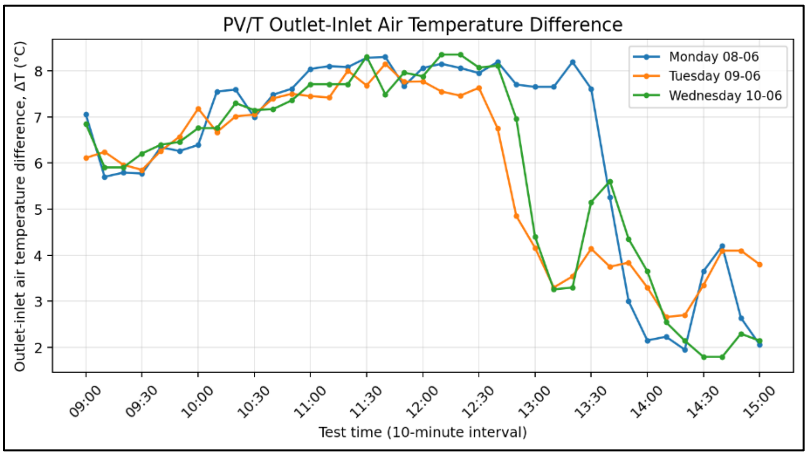

Figure 6. PV/T outlet-inlet air temperature difference at 10-minute intervals.

3.4 Comparison of Indoor and Outdoor Greenhouse Temperatures

The main focus of this revised analysis is the comparison of the air temperature inside the greenhouse and outside the greenhouse. The indoor greenhouse temperature is calculated from the average of DHT5, DHT6, and DHT7, while the outdoor greenhouse temperature is read from DHT8. Figure 7 shows that the temperature inside the greenhouse is generally higher than the outdoor temperature. This difference occurs because the greenhouse functions as an enclosed space that retains heat and receives a supply of hot air from the PV/T outlet. The heat retention mechanism in the greenhouse is also influenced by the enclosure, ventilation, and heat exchange with the environment (Gadhesaria et al., 2020).

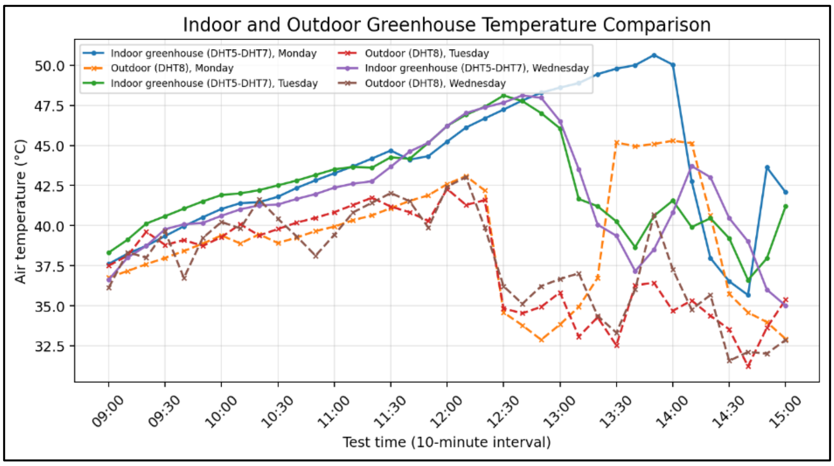

Figure 7. Comparison of indoor greenhouse (DHT5-DHT7) and outdoor greenhouse (DHT8) temperatures.

On Monday, the average greenhouse temperature reached 43.70°C, while the average outdoor temperature was 39.08°C. On Tuesday, the average greenhouse temperature was 42.39°C and the outdoor temperature was

37.66°C. On Wednesday, the average greenhouse temperature was 41.89°C and the outdoor temperature was 37.84°C. Thus, the average indoor-outdoor temperature difference ranges from 4.05°C to 4.73°C. This condition confirms that the hot air from the PV/T and the greenhouse enclosure effect influence the microclimate of the test chamber.

Figure 8. Outdoor greenhouse temperature based on the DHT8 sensor.

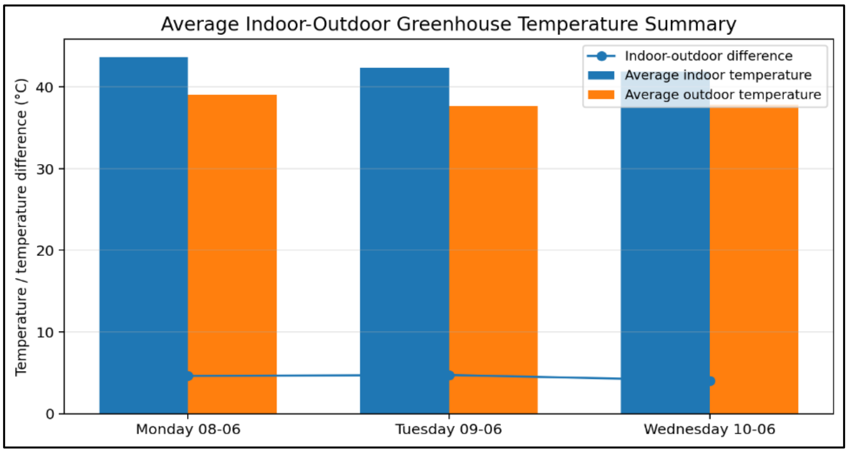

Figure 9. Summary of average indoor-outdoor greenhouse temperatures and their differences.

3.5 Summary of PV/T-Greenhouse Performance

A summary of the measured performance is presented in an integrated table so that the PV/T and greenhouse variables can be evaluated together. Table 4 combines solar radiation, PV/T component temperatures, collector air temperature differences, greenhouse temperatures, outdoor temperatures, and indoor-outdoor temperature differences. Table 5 summarizes the DHT sensor averages, while Table 6 presents the calculated mass flow rate, useful heat transfer, and thermal efficiency.

Table 4. Integrated Summary of PV/T and Greenhouse Performance

Day	n	Avg G (W/m²)	Max G (W/m²)	Avg Bottom PV T (°C)	Avg Absorber T (°C)	Avg Air ΔT (°C)	Max Air ΔT (°C)	Avg T_GH (°C)	Avg Outdoor T (°C)	Avg T_GH - Outdoor (°C)
Monday 08-06	37	768.65	1018	58.07	41.95	6.36	8.30	43.70	39.08	4.62
Tuesday 09-06	37	710.22	959	55.19	39.88	5.81	8.15	42.39	37.66	4.73
Wednesday 10-06	37	676.84	989	55.27	38.99	5.87	8.35	41.89	37.84	4.05

Table 5. DHT Sensor Summary for Indoor and Outdoor Greenhouse Comparison

Day	Avg DHT5 (°C)	Avg DHT6 (°C)	Avg DHT7 (°C)	Avg Outdoor DHT8 (°C)	Avg T_GH (°C)	Difference T_GH - DHT8 (°C)
Monday 08-06	44.65	44.07	42.39	39.08	43.70	4.62
Tuesday 09-06	42.90	43.32	40.96	37.66	42.39	4.73
Wednesday 10-06	41.76	43.34	40.56	37.84	41.89	4.05

3.6 Thermodynamic Performance Calculation

Table 6. Calculated thermodynamic performance of the PV/T air collector.

Day	Avg G (W/m²)	Avg ΔT (°C)	Mass flow rate (kg/s)	Avg useful heat (W)	Thermal efficiency (%)
Monday 08-06	768.65	6.36	0.0774	494.82	24.95
Tuesday 09-06	710.22	5.81	0.0774	452.03	24.67
Wednesday 10-06	676.84	5.87	0.0774	456.70	26.15
Overall average	718.57	6.01	0.0774	467.85	25.24

Calculation basis: ρ_a = 1.184 kg/m³, c_p = 1005 J/kg·K, V_out = 3.70 m/s, outlet duct diameter = 0.15 m, A_o = 0.01767 m², and A_c = 2.58 m².

Based on Tables 4-6, peak solar radiation did not correlate linearly with the most stable maximum greenhouse temperature. The interaction between convective heat transfer from the PV/T outlet and heat retention within the greenhouse enclosure governed this non-linear response. The 4.05°C to 4.73°C indoor-outdoor temperature gradient confirms successful microclimate modification. At a mass flow rate of 0.0774 kg/s, the forced-convection airflow extracted an average of 467.85 W of useful thermal energy and produced an overall average thermal efficiency of 25.24%. The day-specific efficiency was highest on Wednesday (26.15%) because useful heat transfer remained relatively stable despite the lower average solar radiation. Continuous thermal extraction also reduced heat accumulation around the photovoltaic module; however, electrical efficiency was not quantified because electrical output data were not included in the present dataset. The thermal results therefore validate the engineering benefit of integrating an air-based PV/T collector with an agricultural greenhouse (Sadeghi et al., 2022; Wang et al., 2020).

A hotter greenhouse condition compared to the outside environment can be beneficial if the system is directed towards space heating or drying. However, if the system is used for crop cultivation, excessively high temperatures can become a constraint, making it necessary to consider fan settings, ventilation openings, operation times, and airflow control. Thus, the PV/T-Greenhouse system needs to be designed not only to maximize heat utilization but also to maintain microclimate conditions to suit the application needs. For future development, the addition of heat storage or phase change materials can be studied as temperature stabilization options, but these need to be re-tested according to the equipment configuration and operational objectives (Entezari et al., 2026; Naghdbishi et al., 2021).

4. Conclusion

The air-based PV/T-greenhouse system consists of a PV/T collector, an inlet fan, an outlet duct, a greenhouse, T1-T8 thermocouples, DHT1-DHT8 sensors, a radiation sensor, an anemometer, and a data logger. The highest average radiation occurred on Monday, 08-06, at 768.65 W/m², followed by Tuesday, 09-06, at 710.22 W/m², and Wednesday, 10-06, at 676.84 W/m². The average outlet-inlet air temperature difference ranged from 5.81°C to 6.36°C, showing that the PV/T collector consistently increased the outlet air temperature. The calculated mass flow rate was 0.0774 kg/s. Average useful heat transfer was 494.82 W, 452.03 W, and 456.70 W for Monday, Tuesday, and Wednesday, respectively, with an overall average of 467.85 W. The corresponding thermal efficiencies were 24.95%, 24.67%, and 26.15%, giving an overall average of 25.24%. The greenhouse temperature, calculated from DHT- DHT7, remained 4.05°C to 4.73°C above the outdoor temperature recorded by DHT8. These findings demonstrate a quantitatively measurable thermal-management benefit from integrating an air-based PV/T collector with a greenhouse under tropical conditions. Future studies should verify electrical output simultaneously and optimize phase change material integration for thermal stabilization under fluctuating solar radiation.

5. Acknowledgements

The authors express their deepest gratitude to the Mechanical Engineering Study Program, Faculty of Engineering, Universitas Widyatama, for the institutional support and facilities provided during the execution of this research. The highest appreciation is also extended to the supervising lecturers for all the invaluable guidance, evaluations, and discussions from the initial stages of the research to its completion.

The authors also extend special thanks to the Research Center for Energy Conversion Technology, National Research and Innovation Agency (BRIN), for the expert support, research collaboration, and facilities that significantly contributed to the progression of this experimental study. Furthermore, gratitude is directed to all parties, colleagues, and the technical team who have dedicated their time and energy to ensure the smooth process of equipment design, field testing execution, data recording, documentation, up to the drafting stage of this article.

6. Conflict of Interest

The authors declare that they have no known competing financial interests or personal relationships that could have appeared to influence the work reported in this paper.

References

AL-Jaafari, M. A. M., Özalp, M., Abdul Wahhab, H. A., Özarpa, C., & AL-abboodi, H. N. O. (2025). Thermal Efficiency Enhancement of Solar Air Collector Integrated with an Electric Heater Using Experimental and Numerical Approaches. *Sustainability*, *17*(24), 10974. https://doi.org/10.3390/su172410974

Al-Waeli, A. H. A., Kazem, H. A., Chaichan, M. T., & Sopian, K. (2021). A review of photovoltaic thermal systems: Achievements and applications. *International Journal of Energy Research*, *45*(2), 1269–1308. https://doi.org/10.1002/er.5872

Duffie, J. A., Beckman, W. A., & Blair, N. (2020). *Solar Engineering of Thermal Processes, Photovoltaics and Wind*. Wiley. https://doi.org/10.1002/9781119540328

Dunne, N. A., Liu, P., Elbarghthi, A. F. A., Yang, Y., Dvorak, V., & Wen, C. (2023). Performance evaluation of a solar photovoltaic-thermal (PV/T) air collector system. *Energy Conversion and Management: X*, *20*, 100466. https://doi.org/10.1016/j.ecmx.2023.100466

Entezari, S., Khatibi, M., & Sorin, M. (2026). Hybrid photovoltaic–thermal and solar thermal collectors with integrated phase change materials: toward sustainable greenhouse energy systems. *International Journal of Heat and Fluid Flow*, *119*, 110268. https://doi.org/10.1016/j.ijheatfluidflow.2026.110268

Fudholi, A., Musthafa, M. F., Jin, G. L., Darussalam, R., Rajani, A., Setiawan, A., Anwar, A., Yazdi, M. H., Moria, H., Othman, M. Y., Ruslan, M. H., & Sopian, K. (2021). Experimental and model validation of photovoltaic-thermal (PVT) air collector: exergy analysis. *Journal of Mechatronics, Electrical Power, and Vehicular Technology*, *12*(1), 10–17. https://doi.org/10.14203/j.mev.2021.v12.10-17

Fudholi, A., Zohri, M., Taslim, I., Aliyah, F., & Gani Koto, A. (2019). Heat transfer and efficiency of dual channel PVT air collector: a review. *International Journal of Power Electronics and Drive Systems (IJPEDS)*, *10*(4), 2037. https://doi.org/10.11591/ijpeds.v10.i4.pp2037-2045

Gadhesaria, G., Desai, C., Bhatt, R., & Salah, B. (2020). Thermal Analysis and Experimental Validation of Environmental Condition Inside Greenhouse in Tropical Wet and Dry Climate. *Sustainability*, *12*(19), 8171. https://doi.org/10.3390/su12198171

Geary, D. F. (2014). American Society of Heating, Refrigerating and Air-conditioning Engineers Guideline 12-2000: Minimizing the Risk of Legionellosis Associated with Building Water Systems. In *Legionella* (pp. 376–384). ASM Press. https://doi.org/10.1128/9781555817985.ch77

Gorjian, S., Hosseingholilou, B., Jathar, L. D., Samadi, H., Samanta, S., Sagade, A. A., Kant, K., & Sathyamurthy, R. (2021). Recent Advancements in Technical Design and Thermal Performance Enhancement of Solar Greenhouse Dryers. *Sustainability*, *13*(13), 7025. https://doi.org/10.3390/su13137025

Jadallah, A. A., Alsaadi, M. K., & Hafidh, Z. A. (2020). Innovative Design of a Ventilated Modern Greenhouse Powered by PV/T Solar System. *IOP Conference Series: Materials Science and Engineering*, *765*(1), 012040. https://doi.org/10.1088/1757-899X/765/1/012040

Naghdbishi, A., Yazdi, M. E., & Akbari, G. (2021). Numerical study on the performance of a glazed photovoltaic thermal system integrated with phase change material (GPVT/PCM): on the contribution of PCM volumetric fraction and environmental temperature. *Renewable Energy*, *172*, 1060–1074.

Sadeghi, G., Mehrali, M., Shahi, M., Brem, G., & Mahmoudi, A. (2022). Progress of experimental studies on compact integrated solar collector-storage retrofits adopting phase change materials. *Solar Energy*, *237*, 62–95. https://doi.org/10.1016/j.solener.2022.03.070

Wang, X., Xia, L., Bales, C., Zhang, X., Copertaro, B., Pan, S., & Wu, J. (2020). A systematic review of recent air source heat pump (ASHP) systems assisted by solar thermal, photovoltaic and photovoltaic/thermal sources. *Renewable Energy*, *146*, 2472–2487. https://doi.org/10.1016/j.renene.2019.08.096

Zhou, D., Zhai, P., Liu, X., Hu, G., & Li, R. (2025). Annual optimal performance analysis of PV/T inside and outside greenhouse in northwest China. *Case Studies in Thermal Engineering*, *73*, 106457. https://doi.org/10.1016/j.csite.2025.106457